

## A Numerical Experiment on the Inter-annual Variation Induced by the Current in a Basin with Dimension Comparable to the East Sea

Kyoung-Ho Cho and Young Ho Seung\*

Department of Oceanography, Inha University, Incheon 402-751, Korea

(Received July 2000, Accepted September 2000)

A series of numerical experiments are performed to examine the generation of inter-annual variations by an inertial current in an idealized semi-enclosed basin with dimension comparable to that of the East Sea. Model results indicate that the inter-annual variations dominate the kinetic energy spectrum with a peak around the time scales of 2~3 years. These variations are mostly due to the westward propagating meanders and large eddies induced by the instability of current, indicating their dependency on the eddy-resolving capacity of the model. They are generated in the interior of the basin but their energy is largely confined near the western boundary such that the east-west dimension of the basin cannot be considered as a critical factor as long as the basin covers enough western boundary region. Overall, this study suggests that the inter-annual variation observed in the East Sea is due to the meandering and large eddies induced by the instability of the current.

Key words: inter-annual variation, numerical experiment

### Introduction

It is only recently that many attentions have been paid on inter-annual variations present in the ocean. Except those related with the ENSO in the tropical region, the mechanism of these inter-annual variations are not well understood. Hirose and Ostrovskii (2000) found fluctuations of sea surface elevation with period of about two years from the altimetry data. With surface elevation data assimilated, his reduced gravity model shows the similar variation. An inter-annual variation of kinetic energy, with period of about 3~4 years, is also remarked by Holloway et al. (1995) in his relatively coarse-grid numerical model for the case of steady wind forcing. With annual wind forcing, however, this fluctuation is greatly dominated by the annual fluctuation. Since then, no further information about these inter-annual variations is provided.

One of the candidate generation mechanisms of these inter-annual variations is the instability of the current such as meanders and eddies. To test this idea, a numerical experiment is performed with idealized model basin. The advantages of using the

idealized model are two fold. First, it is much easier than the realistic simulation because of its simplicity; numerical modeling of the East Sea has experienced much progress until now (e.g., Yoon, 1982a, 1982b and 1982c; Seung and Kim, 1993; Kim et al., 1997; Kim and Yoon, 1999; Kim and Seung, 1999) but still there are many problems to be solved, especially the uncertainty in the surface and open boundary conditions. Second, it excludes many other factors affecting the inter-annual variation making it easier to extract the candidate mechanism; as noted by Holloway et al. (1995), the seasonality of forcings is expected to greatly mask the inter-annual variation. Overall, the purpose of this study is to propose for the first time that the inter-annual variation recently observed in the East Sea is a manifestation of the current instability which generates westward propagating eddy-like disturbances.

### Model

A simple reduced-gravity model is used in this study. The upper layer thickness is taken initially as 250 meters. The relative density difference between the upper and the lower motionless layers,  $\Delta\rho/\rho$ , is

\*To whom correspondence should be addressed.

taken as  $1.5 \times 10^{-3}$ . Since the reduced-gravity model produces only the lowest vertical mode, the effects of other higher vertical modes and bottom topography are not considered. The model is based on the Miami Isopycnic Coordinate Ocean Model (Bleck et al., 1992) version 2.5 adapted to the model basin. Since the original mixed layer dynamics is ignored here, the thermodynamic effect occurring at the basin surface is absent. A rectangular model domain is considered extending from  $130.05^\circ\text{E}$  to  $139.05^\circ\text{E}$  and from  $34.4^\circ\text{N}$  to  $48.0^\circ\text{N}$  with grid size 0.1 by 0.1 degrees in latitude and longitude. A current is driven by an inflow with transport 2 Sverdrups. Outflow transport is self determined depending on the interior conditions near the outflow opening as described by Seung and Cho (1998). The inflow opening is located from  $130.23^\circ\text{E}$  to  $130.77^\circ\text{E}$  on the southern boundary and the outflow opening, from  $43.32^\circ\text{N}$  to  $43.59^\circ\text{N}$  on the eastern boundary. As the eddy viscosity formulation, the biharmonic scheme is used to enhance the eddy-resolving capacity in which the viscosity is taken to be proportional to the absolute value of the total deformation of horizontal motion

field (Smagorinsky, 1963). As the proportionality factor,  $\lambda$ , two values, 0.04 and 1.0, are considered to examine the dependence of the inter-annual variation on the eddy-resolving capacity of the model. Although there is not any absolute criteria on the relationship between the magnitude of  $\lambda$  and the eddy-resolvability, these two values are considered to be approximately the upper and lower limit for the eddy-resolving capacity with smaller one having larger capacity. All the models considered in this study is numbered for convenience and parameters used in each model are shown in Table 1.

Table 1. Parameters used in each of four model run (numbered)

Run number	E-W basin dimension (km)	Proportionality factor of viscosity $\lambda$
1	1000	0.04
2	1000	1.0
3	500	0.04
4	2000	0.04

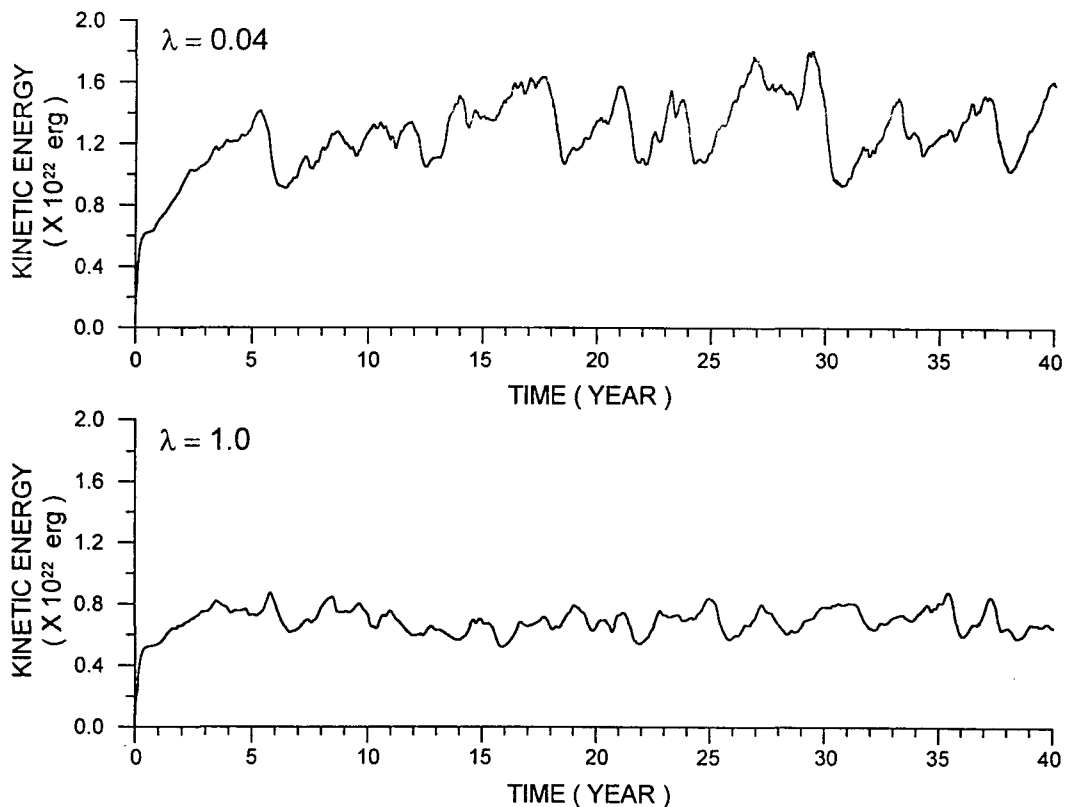


Fig. 1. Time serieses of total kinetic energy for two different eddy viscosity represented by two different proportionality factors ( $\lambda$ ).

Results

Time series of total kinetic energy obtained for the basin with east-west dimension of about 1000 km indicates that statistically steady states are reached after 10 years of run (Fig. 1). The time series of total kinetic energy clearly shows an inter-annual variation at period of more than one year as remarked by

Holloway et al. (1995) and by Hirose and Ostrovskii (2000). Time scales of inter-annual variation obtained in these studies and in our model are slightly different each other. Since these time scales can vary slightly depending on model circumstances, perhaps that by Hirose and Ostrovskii may be most reliable. As expected, the result with smaller eddy viscosity (smaller  $\lambda$ , run 1) shows more energy than the other.

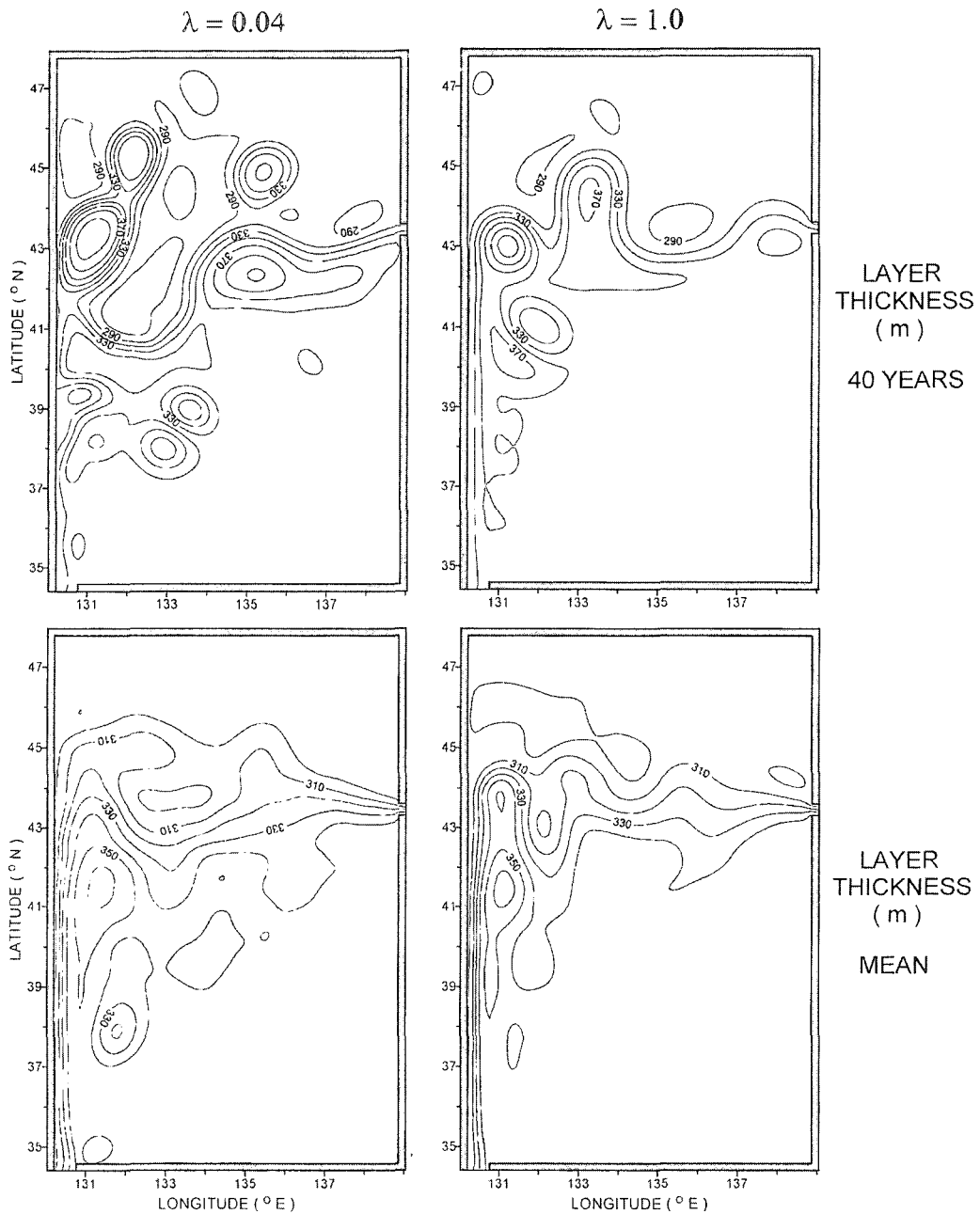


Fig. 2. Horizontal distributions of layer thickness for two different proportionality factors of eddy viscosity  $\lambda$ : snapshot at the 40 years of run (upper panel) and average over the period of 30~40 years (lower panel).

This fact indicates that the non-linear interaction of current with small-scale disturbances interferes in the generation of the inter-annual variation, although this effect cannot be quantified. As seen from the snapshot of layer thickness distribution at 40 years of run (Fig. 2), more eddies are generated for smaller eddy viscosity (note that currents are largely geostrophic such that they run parallel to the isopleths

of the layer thickness as seen by comparing Fig. 2 with Fig. 3). The mean currents averaged over the period of 30~40 years, however, appear similar to each other, *i.e.*, they form western boundary currents and, after separating from the coast, flow toward the outflow opening nearly zonally (Fig. 2). The predominance of the inter-annual variation is confirmed in the spectra of total kinetic energy (Fig. 4). As

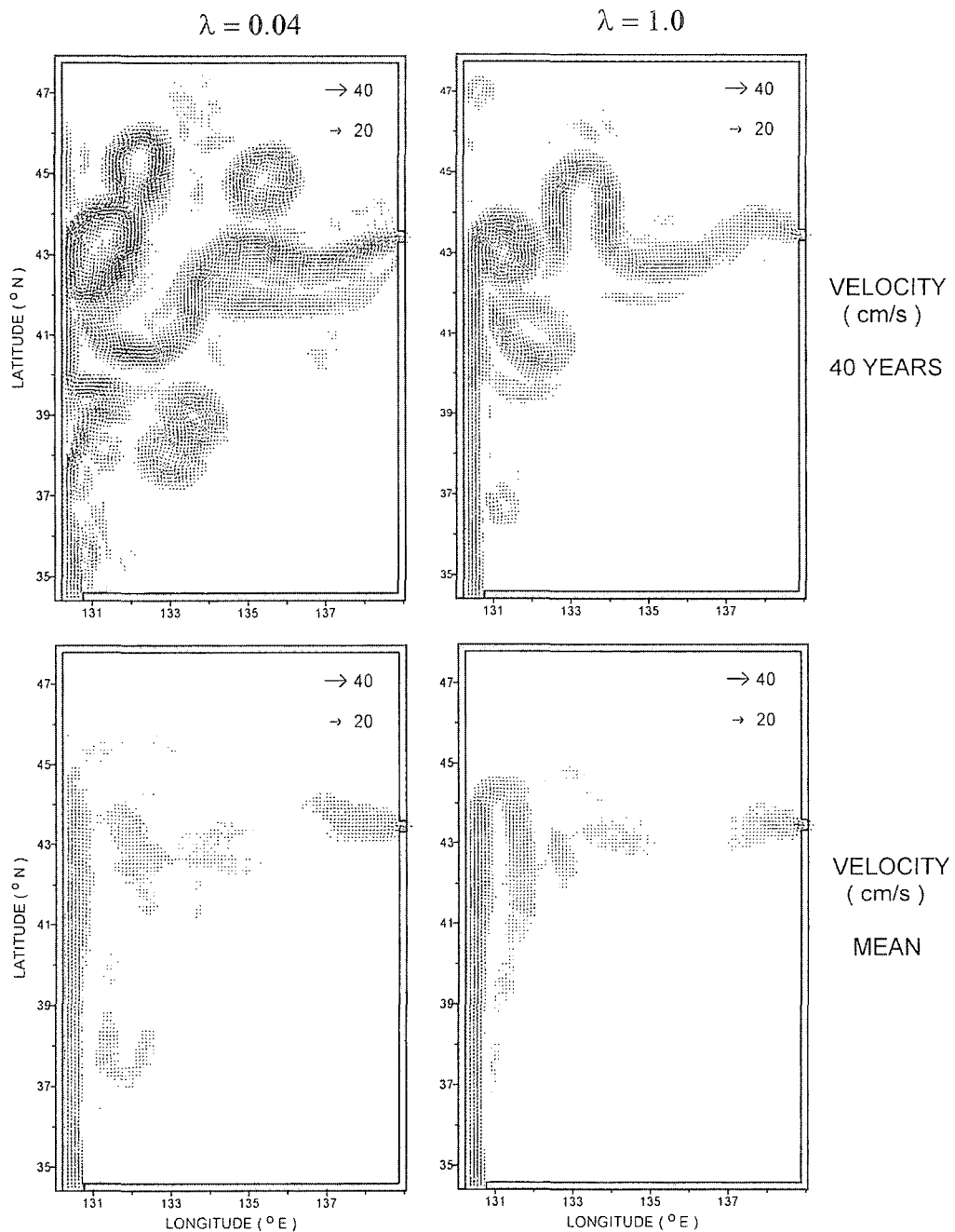


Fig. 3. Horizontal distributions of current vector corresponding to the layer thickness shown in Fig. 2.

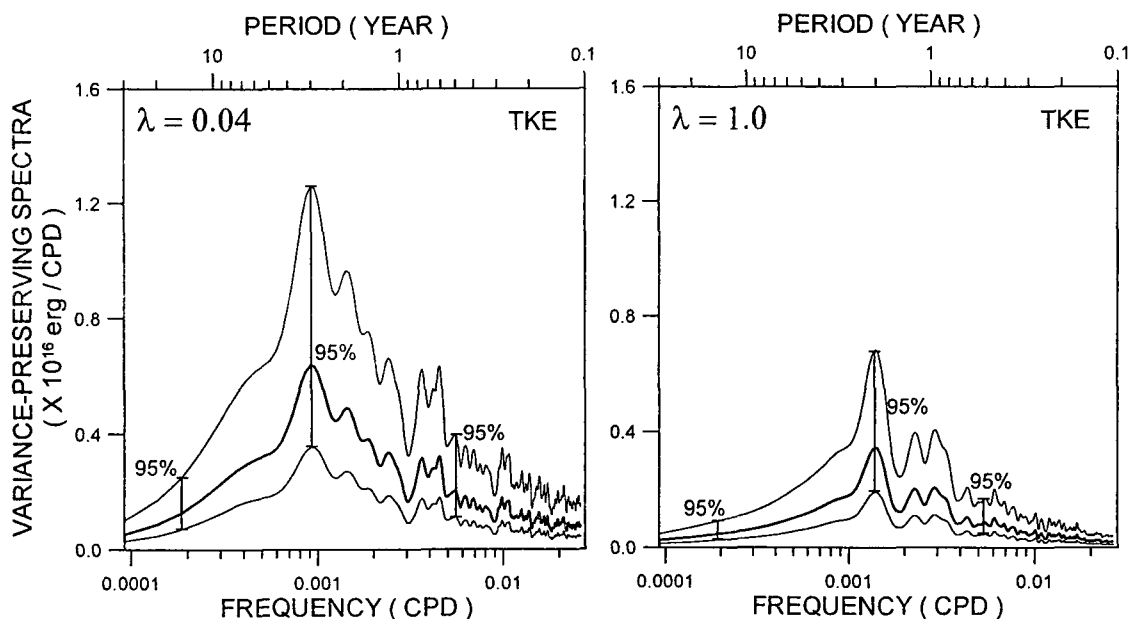


Fig. 4. Spectra of total kinetic energy (TKE) for two different proportionality factors of eddy viscosity  $\lambda$  (thick line at the center). Upper and lower thin lines represent 95% confidence limits. Parzen window is used in smoothing the periodograms.

noted above, the result with smaller eddy viscosity has more energy than the other.

Current velocities and layer thickness are low-pass filtered for time scales larger than two months over the period of 30~40 years. The resulting variances are distributed as shown in Figure 5. It indicates that the low-frequency energy which is dominated by the inter-annual variation is largely confined near the western boundary, especially near the separation point of the western boundary current. Time-space diagrams of the layer thickness, and east and north components of current velocity obtained along the latitude line  $41.6^\circ\text{N}$  indicate that the inter-annual variation is most probably related with the westward propagation of disturbances (Fig. 6). The propagation speed is about 270 and 300 km/year for run 1 and 2 respectively, which are quite comparable to the propagation speed of long internal Rossby waves. The latter is given by  $\beta R^2$  ( $\sim 278$  km/year) with  $\beta$  ( $\sim 2 \times 10^{-11}$   $\text{sec}^{-1} \text{m}^{-1}$ ) and  $R$  ( $= \sqrt{g'H}/f \sim 21$  km with  $g' \sim 1.5 \times 10^{-2}$   $\text{m sec}^{-2}$  the reduced gravity,  $H \sim 300$  m the mean layer thickness (*c.f.*, Fig. 2) and  $f \sim 10^{-4}$   $\text{sec}^{-1}$  the Coriolis parameter), respectively, the meridional gradient of Coriolis parameter and the internal Rossby radius. With this speed and the time scale of 2~3 year, the scale of inter-annual variation can be estimated as about 540~900 km.

Since the scale of inter-annual variation is comparable to the east-west basin scale, which is about 1000 km, the basin scale might be a parameter affecting the inter-annual variation. To answer this question, another two experiments are performed for two different model basins, one with the east-west dimension two times smaller ( $\sim 500$  km, run 3) and the other, two times larger ( $\sim 2000$  km, run 4) than that considered above. The proportionality factor of eddy viscosity is taken as 0.04. The resulting spectra do not appear quite different from the standard one (Fig. 7). This may come from the fact that most energy is trapped near the western boundary (Fig. 8). However, the nature of westward propagation appears quite different for the basin with smallest dimension (Fig. 9). For this case, disturbances lose much of the propagating wave character while gaining much of the standing wave character. This may be caused by the constraint imposed by the lateral boundaries. However, this problem is beyond the scope of present study and further discussions cannot be proceeded.

### Concluding Remarks

An idealized simple model considered here suggests that the inter-annual variation observed in the East

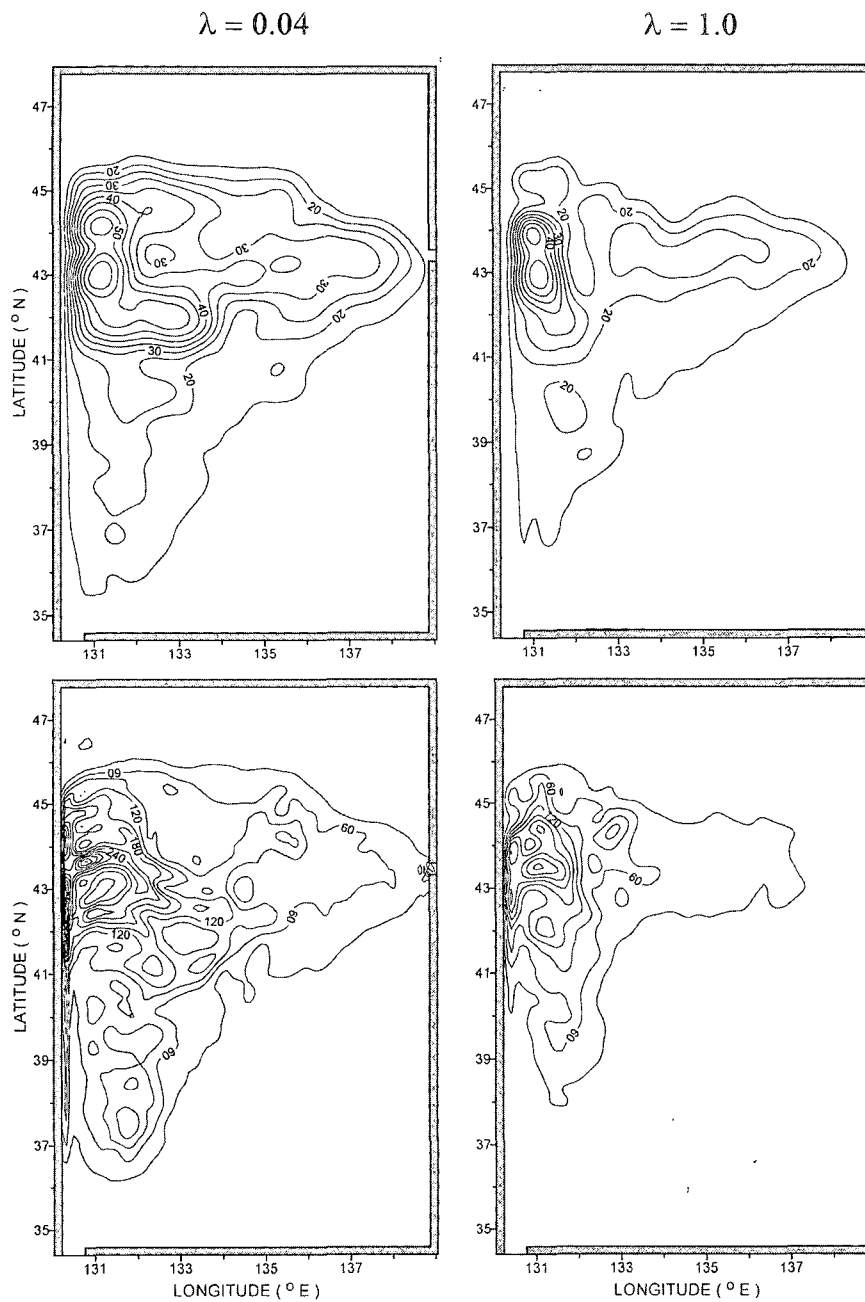


Fig. 5. Variance distributions of low-frequency fluctuations of layer thickness (upper panel) and current velocity (lower panel) for two different proportionality factors of eddy viscosity  $\lambda$ .

Sea is due to the meandering and large eddies induced by the instability of the current. It is possible that the inter-annual variations may be masked by other effects such as the seasonally fluctuating wind forcing as noted by Holloway et al. (1995), although they have been successfully detected by Hirose and Ostrovskii (2000). Holloway et al. (1995) obtained the inter-annual variation with relatively coarse-gridded

and diffusive model. Were it for more eddy-resolving capacity, more energetic inter-annual variation may have been resulted, perhaps even with the seasonally varying wind forcing. The inter-annual variation can also be affected by the air-sea heat exchange and bottom topography. All these factors should ultimately be considered with more complete model to examine the realistic inter-annual variation of the East Sea.

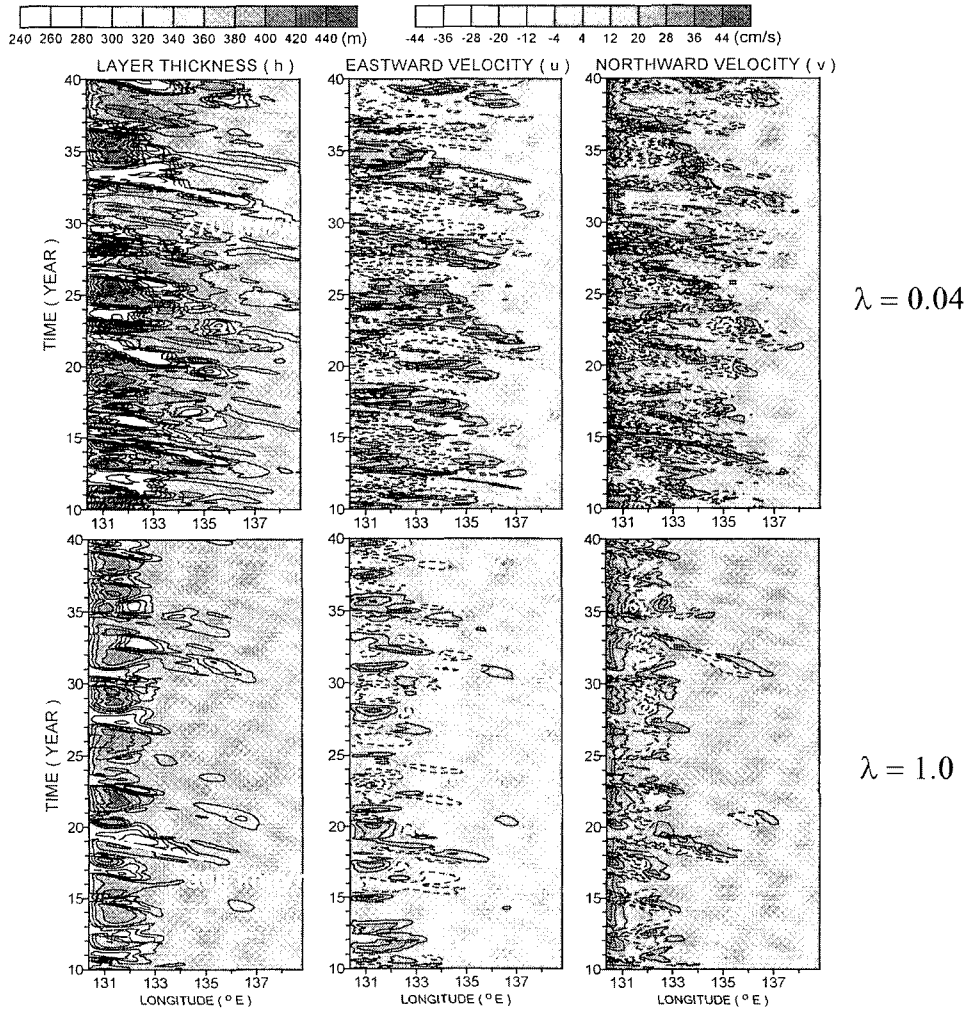


Fig. 6. Time-space diagrams of layer thickness,  $h$ , and two components of current velocity,  $u$  and  $v$ , taken along the latitude  $41.6^\circ\text{N}$  for two different proportionality factors of eddy viscosity  $\lambda$ .

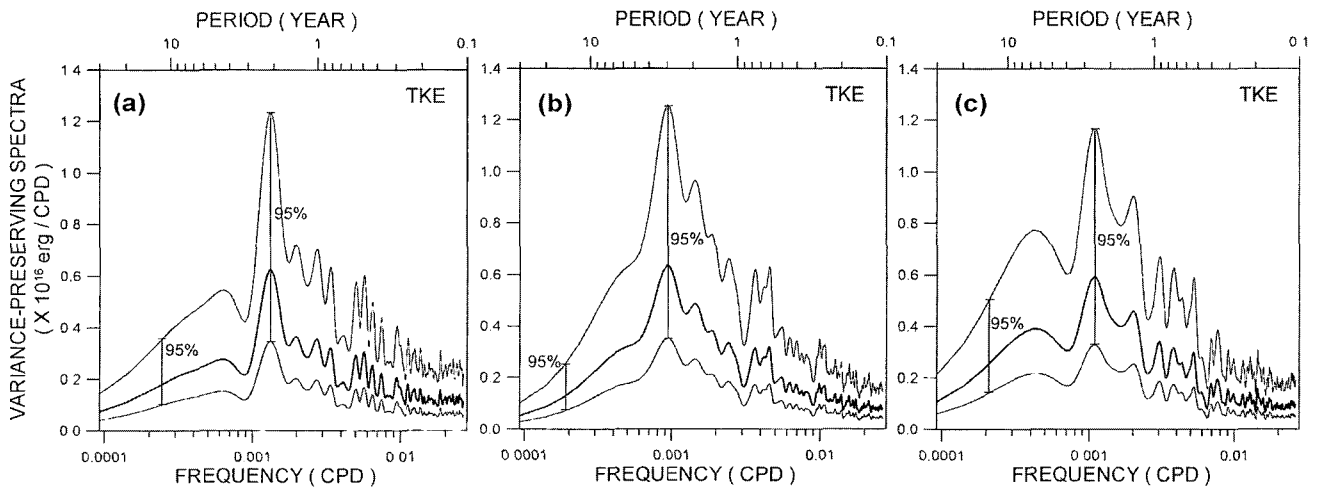


Fig. 7. Spectra of total kinetic energy for three model basins with different east-west dimensions: (a), the smallest ( $\sim 500$  km); (b), the standard ( $\sim 1000$  km); and (c), the largest ( $\sim 2000$  km) dimension.

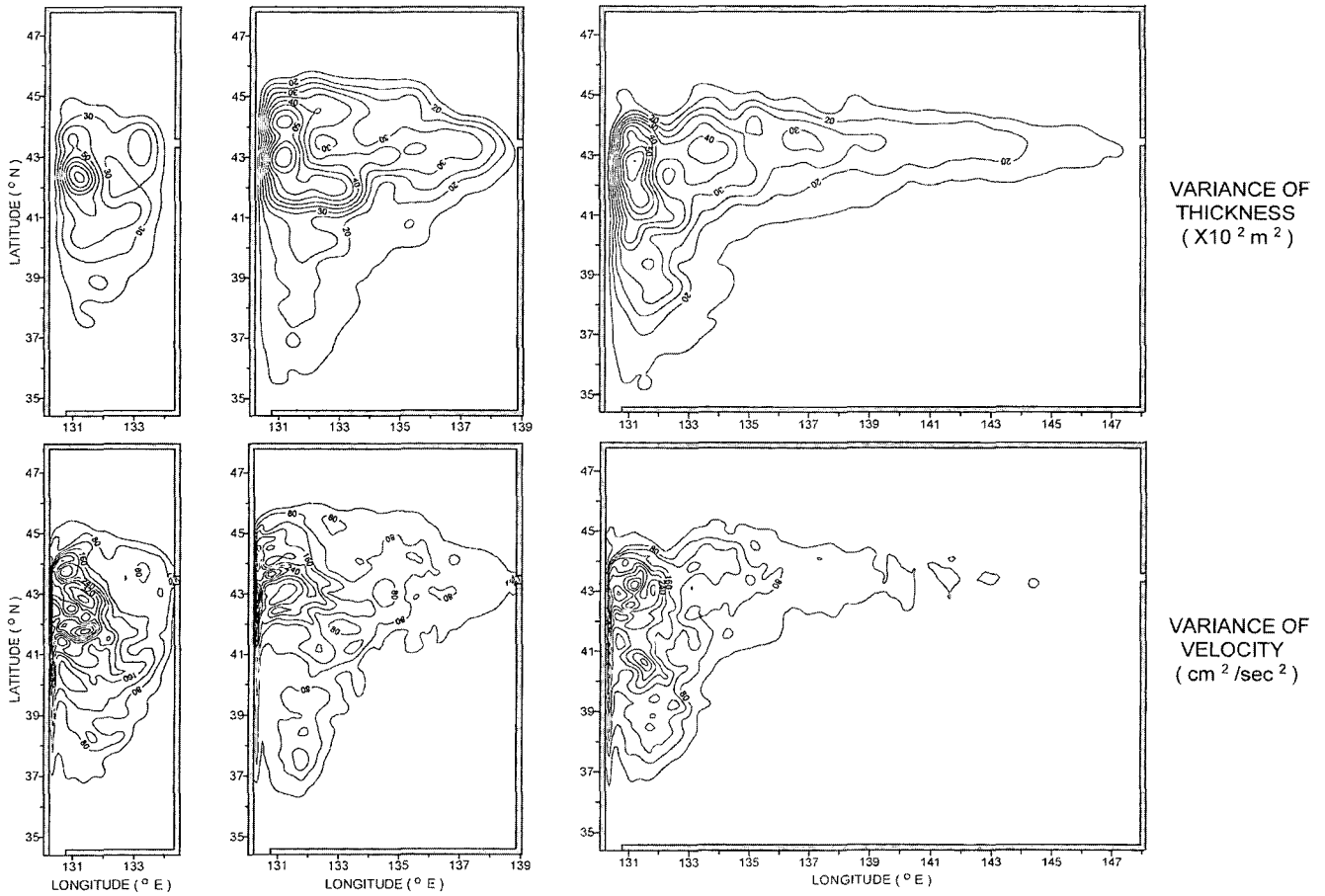


Fig. 8. Variance distributions of low-frequency fluctuations of layer thickness (upper panel) and current velocity (lower panel) for three model basins with different east-west dimensions.

Although this study is only a first step toward this goal, it strongly indicates that the key factor to understand the generation mechanism of the inter-annual variation in the East Sea is the non-linear instability of the circulation.

### Acknowledgements

This study is supported by the Korea Research Foundation (1998). Kind comments by an anonymous reviewer are greatly appreciated.

### References

- Bleck, R., C. Rooth, D. Hu and L.T. Smith. 1992. Salinity-driven thermocline transients in a wind- and thermohaline-forced isopycnic coordinate model of the North Atlantic. *J. Phys. Oceanogr.*, 22, 1486~1505.
- Hirose, N. and A.G. Ostrovskii. 2000. Quasi-biennial variability in the Japan Sea. *J. Geophys. Res.*, 105, 14011~14027.
- Holloway, G., T. Sou and M. Eby. 1995. Dynamics of circulation of the Japan Sea. *J. Mar. Res.*, 53, 539~569.
- Kim, S.Y., J.C. Lee, H.S. Lee and T.B. Shim. 1997. Triggering effect of the polar front on the eddies in the East Sea. *J. Korean Fish. Soc.*, 30, 1044~1055.
- Kim, C.H. and J.H. Yoon. 1999. A numerical modeling of the upper and the intermediate layer circulation in the East Sea. *J. Oceanogr.*, 55, 327~345.
- Kim, K.J. and Y.H. Seung. 1999. Formation and movement of the ESIW as modeled by MICOM. *J. Oceanogr.*, 55, 369~382.
- Smagorinsky, J.S. 1963. General circulation experiments with the primitive equations: I. The basic experiment. *Mon. Wea. Rev.*, 91, 99~164.
- Seung, Y.H. and K. Kim. 1993. A numerical modeling of the East Sea circulation. *J. Oceanol. Soc. Korea*, 28, 292~304.
- Seung, Y.H. and K.-H. Cho. 1998. A note on the outflow boundary conditions in modeling the East Sea circulation. *J. Korean Soc. Oceanogr.*, 33, 212~218.
- Yoon, J.H. 1982a. Numerical experiment on the circulation in the Japan Sea. Part I. Formation of the East Korean Warm Current. *J. Oceanogr. Soc. Japan*, 38, 43~51.



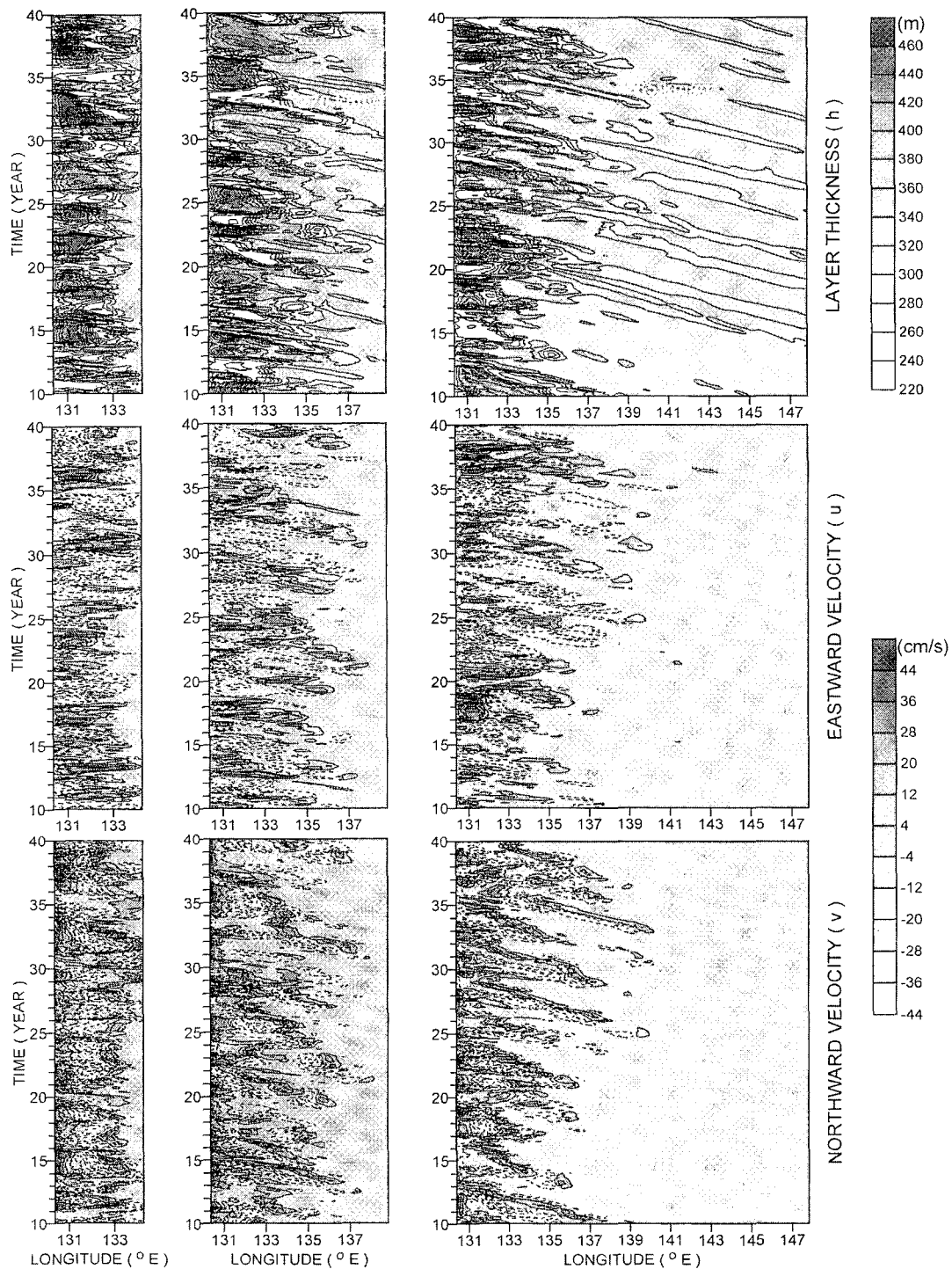


Fig. 9. Time-space diagrams of layer thickness,  $h$ , and two components of current velocity,  $u$  and  $v$ , taken along the latitude  $41.6^\circ\text{N}$  for three model basins with different east-west dimensions.

Yoon, J.H. 1982b. Numerical experiment on the circulation in the Japan Sea. Part II. Influence of seasonal variations in atmospheric conditions on the Tsushima Current. *J. Oceanogr. Soc. Japan*, 38, 81~94.

Yoon, J.H. 1982c. Numerical experiment on the circulation in the Japan Sea. Part III. Mechanism of the Nearshore Branch of the Tsushima Current. *J. Oceanogr. Soc. Japan*, 38, 125~130.